Proceedings of CONF-MCEE 2026 Symposium: Advances in Sustainable Aviation and Aerospace Vehicle Automation
DOI: 10.54254/2755-2721/2026.KA26760

Cascade Control Strategies for Power Electronic Transformers

Xinyu Wu

School of Electrical Engineering, China University of Mining and Technology, Xuzhou, China
xinyuwu57@qq.com

Abstract. Power Electronic Transformer (PET) is widely applied in smart grids, renewable energy, rail transit and other fields for its integrated functions of voltage conversion, electrical isolation and power quality control. With the development of wide-bandgap semiconductor materials such as SiC and GaN, as well as digital control technology, PET has gradually replaced traditional transformers and played a significant role in scenarios like flexible AC/DC hybrid power grids. This paper sorts out the control strategies of PET from three dimensions: modulation technology, voltage and power balancing control strategies, and port control technologies. Finally, it summarizes and prospects the current technical challenges and future development trends of PET.

Keywords: Power Electronic Transformer, Modulation Techniques, Voltage and Power Balancing Control Strategies, Port Control Technologies

1. Introduction

Power Electronic Transformer (PET) is realized via power electronic technology and high-frequency transformers. Compared with traditional transformers, PET boasts multiple functions including voltage transformation, electrical isolation, power regulation and control, and renewable energy integration [1]. It also features high controllability, and enables control over waveform, power flow and power quality, as well as automatic protection control [2].

In recent years, PET technology has developed rapidly with various topologies proposed. Among them, the most extensively studied topology is the three-stage PET topology shown in Figure 1. This topology model consists of three parts: H-bridge rectifier, Dual Active Bridge (DAB) DC-DC converter and inverter.

© 2026 The Authors. This is an open access article distributed under the terms of the Creative Commons Attribution License 4.0 (https://creativecommons.org/licenses/by/4.0/).

DOI: 10.54254/2755-2721/2026.KA26760

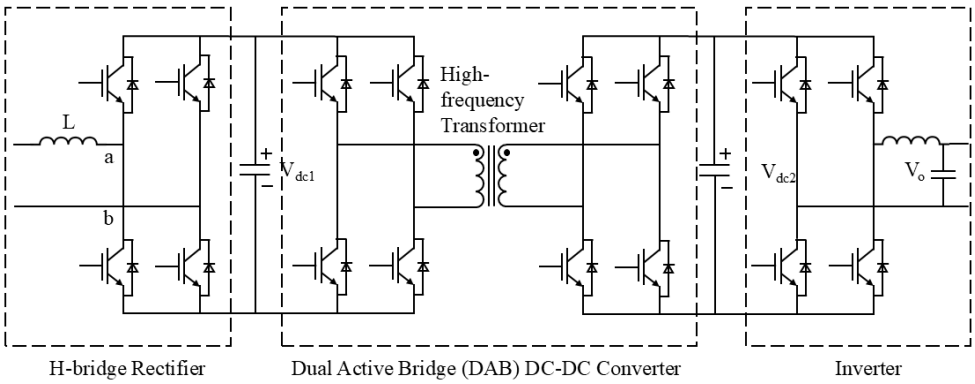

Figure 1. Three-stage power electronic transformer [3]

Each part of the multi-stage PET has sound independence, which avoids the direct AC/AC link and improves control flexibility [4, 5], endowing it with great application potential in connecting various types of power sources, loads and energy storage devices. Therefore, as PET topology development has gradually matured, domestic and foreign scholars have shifted their research focus to the optimization of control strategies for three-stage PET [4].

This paper sorts out and summarizes the key technical literature on the control strategies of three-stage PET, and divides the content into three parts. Section 1 introduces modulation technologies, including control strategies for the input stage and the intermediate-stage DAB; Section 2 introduces voltage balancing and power balancing technologies; Section 3 introduces port control technologies under multi-load access conditions; Section 4 summarizes the development status of cascaded PET and concludes the optimization direction of its control strategies.

2. Modulation technologies for cascaded power electronic transformers

Cascaded PET usually adopts a three-stage structure: input stage, intermediate stage and output stage. As the first stage of the entire PET, the input stage is mainly responsible for converting AC grid input into the power form required by the intermediate stage. Common input stage topologies include Multilevel Cascaded H Bridge (MLCHB) rectifier and Modular Multilevel Converter (MMC) rectifier. The intermediate-stage DAB is a high-frequency isolated DC-DC converter topology widely used in PET, electric vehicle charging, renewable energy systems and energy storage systems, known for its high efficiency, high power density and bidirectional power flow capability.

Among input stage topologies, MLCHB has become a research hotspot for its excellent current harmonic performance, high-voltage endurance and high modular structure. Compared with the basic CHB structure, MLCHB adds more H-bridge units to achieve more level outputs, with expanded application scenarios. It is commonly used in high-voltage direct current (HVDC) transmission, high-power motor drives and power quality improvement equipment, featuring easy implementation, high reliability, low harmonics and small distortion [6]. MMC features a modular design with each sub-module independently controllable. Similar to MLCHB, it is mostly applied in high-voltage scenarios and has attracted wide attention as a voltage-source converter for the engineering implementation of flexible DC transmission [7].

DOI: 10.54254/2755-2721/2026.KA26760

2.1. Input stage

For several input stage structures, the most common modulation methods are Phase Shifted Carrier Pulse Width Modulation (PSC-PWM) and Space Vector Pulse Width Modulation (SVPWM). Both can realize sound control over MLCHB and MMC rectifiers. The following part focuses on these two input-stage modulation methods and elaborates on the control strategies under different topologies.

2.1.1. Phase Shifted Carrier Pulse Width Modulation (PSC-PWM)

Carrier phase-shifted pulse width modulation is based on the carrier phase-shift method. It uses multiple triangular carriers with identical amplitude and respective phase shifts to compare with the modulation wave, generates PWM waves to control each power unit separately, and then superimposes them to form a multi-level PWM wave [8]. Through carrier phase-shift modulation, changing the phase of high-frequency current harmonics output by the converter can greatly reduce the current harmonics at the output stage [9, 10]. Meanwhile, it enables sub-modules in the modular structure to synthesize a higher equivalent switching frequency at the AC terminal with the same low switching frequency, thus improving the output waveform quality.

Reference [11] takes a three-level H-bridge inverter as the research object and conducts experimental research on the abnormal increase of neutral line current when applying carrier phase-shift modulation. The fifteen-phase three-level H-bridge inverter uses voltage pulse sequences instead of reference voltages. Due to the asymmetric voltage of each bridge arm of the inverter, an alternating high-frequency common-mode voltage is formed between the stator windings of the load motor. Meanwhile, a closed common-mode loop is formed through various distributed and parasitic capacitances in the whole motor system. The high-frequency common-mode voltage drives periodic charge movement among parasitic capacitances via the common-mode loop, thus generating common-mode current [11]. By calculating the circulating current amplitude, the curves of three channels varying with the inter-channel carrier phase shift angle θ are obtained (Figure 2). It can be seen that the neutral line current increases sharply after the carrier phase shift is applied.

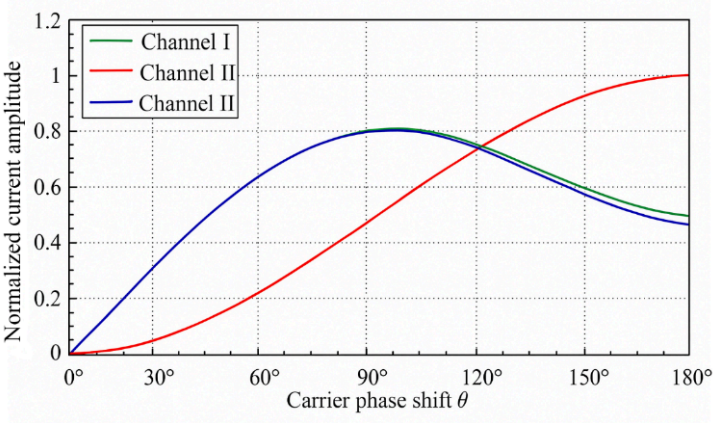

Figure 2. The theoretical calculation value of the neutral line circulation amplitude variation curve of the three channels of the inverter [11]

Analysis shows that the root cause lies in the ground potential difference at the midpoint of each channel, and the circulating current amplitude can be suppressed by reducing the common-mode voltage amplitude. By deriving the midpoint potential expression, the curve of midpoint potential

DOI: 10.54254/2755-2721/2026.KA26760

amplitude varying with the carrier phase shift angle is obtained (Figure 3). It shows that the amplitude reaches the minimum when the carrier phase shift angle is 72°, thus realizing the suppression of neutral line current [11].

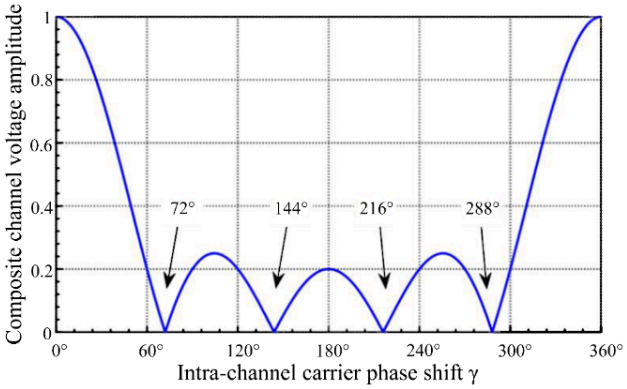

Figure 3. The curve of the amplitude of five-phase synthetic potential in a single channel of the inverter with the phase shift angle of the five-phase carrier in the channel [11]

Modular multilevel rectifier (MMC) is another common topology. Reducing switching frequency and eliminating circulating current in the voltage balancing of cascaded sub-module (SM) capacitors are two core problems for MMC. Reference [12] introduces an improved PSC-PWM scheme for MMC based on a reduced switching frequency (RSF) voltage balancing algorithm.

PSC-PWM can automatically suppress all low-order harmonics of multi-level converters. However, in the traditional PSC-PWM method, each carrier corresponds to the switching mode of a single SM. Due to the different characteristics of each SM, dynamic voltage imbalance occurs among SM DC capacitors. The RSF algorithm is adopted to improve PSC-PWM, and Figure 4 shows the schematic diagram of modulation and balancing control. As shown in the figure, there are two control frequencies: *f*cr for carrier frequency and *f*s for sampling and control frequency.

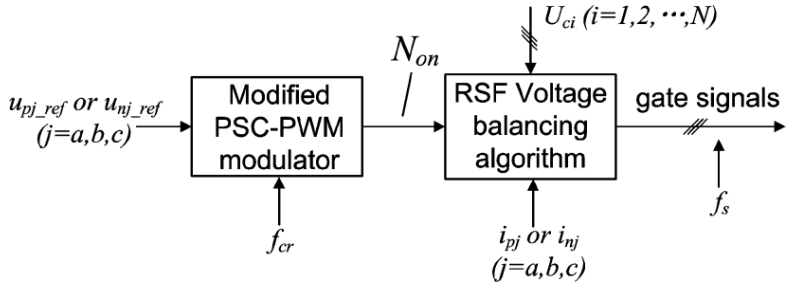

Figure 4. Entire modulation and balancing control schemes [12]

The improved PSC-PWM method is illustrated in Figure 5. According to the number N of SMs per arm, the reference arm voltage is compared with N triangular carriers with a phase difference of 360°/N between each other. *N*on, the number of SMs to be turned on per arm, serves as the output of the modulator.

DOI: 10.54254/2755-2721/2026.KA26760

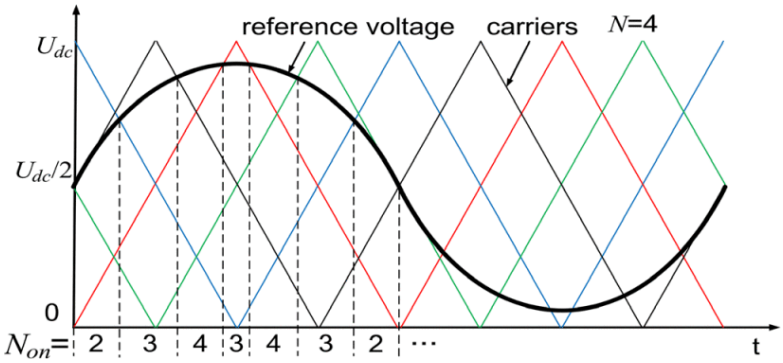

Figure 5. Modified PSC-PWM method [12]

SMs are selected based on the RSF algorithm, and switching pulses are generated by monitoring the SM capacitor voltage *U*ci (*i*=1,2,…,N) and the direction of arm current *i*cj or *i*nj (*j*=1,2,…,N). To avoid excessive switching frequency, the literature improves the traditional RSF algorithm. As shown in Figure 6, the switching principle of the algorithm is summarized as follows:

1. If additional sub-modules need to be turned on in the next control cycle, the currently on-state sub-modules will not perform any switching operation.

2. If some currently on-state sub-modules need to be turned off in the next control cycle, no additional currently off-state sub-modules will be turned on.

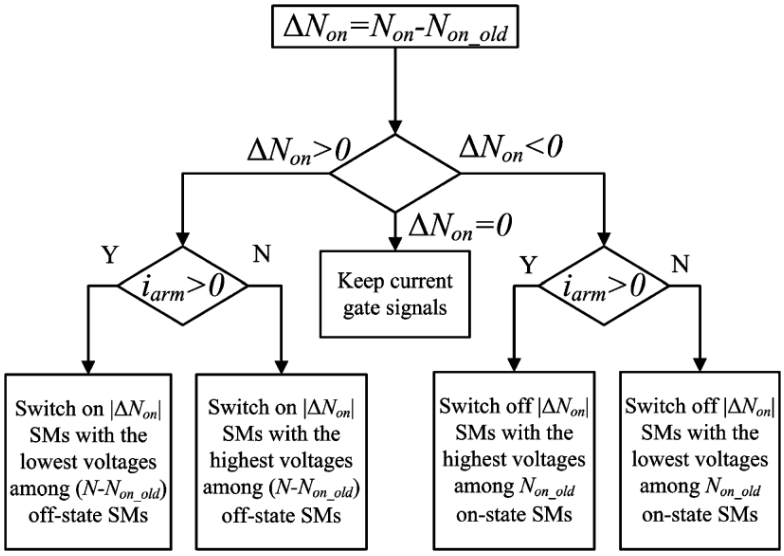

Figure 6. Reduced switching-frequency (RSF) voltage-balancing algorithm [12]

Compared with traditional methods, the proposed RSF voltage balancing algorithm significantly reduces the average switching frequency of devices and the total switching loss of the converter.

2.1.2. Space Vector Pulse Width Modulation (SVPWM)

The traditional method of generating PWM by comparing high-frequency triangular waves with modulation waves is more suitable for analog circuits and unfavorable for digital implementation [13]. Therefore, SVPWM is developed as a digital alternative to SPWM. Reference [13] proves that SVPWM achieves the highest DC voltage utilization by analyzing the principle of voltage space vector.

DOI: 10.54254/2755-2721/2026.KA26760

For its easy digital implementation and high voltage utilization, SVPWM is widely adopted as the modulation algorithm in voltage-source inverters. Reference [14] proposes a three-level SVPWM modulation method with neutral-point potential balancing function. Among traditional SVPWM neutral-point potential control methods, the most common one is adjusting the action time of redundant small vectors via hysteresis control. The effect of this scheme is highly related to power factor: the lower the power factor, the less satisfactory the neutral-point control effect. The traditional control scheme is improved by utilizing the feature that redundant small vectors appear in pairs, with each pair generating the same line voltage and opposite neutral-point current. To verify the effectiveness of the algorithm, a three-level inverter experimental platform with TMS320LF2407A DSP as the core control chip is built for simulation tests, and the simulation waveform of neutral-point voltage balancing control is obtained. As clearly shown in Figure 7, before t=0.04s when no neutral-point control is applied, both the output PWM phase voltage amplitude and the neutral-point voltage fluctuation waveform show large fluctuations; after the neutral-point algorithm is added, the voltage fluctuation is effectively suppressed [14].

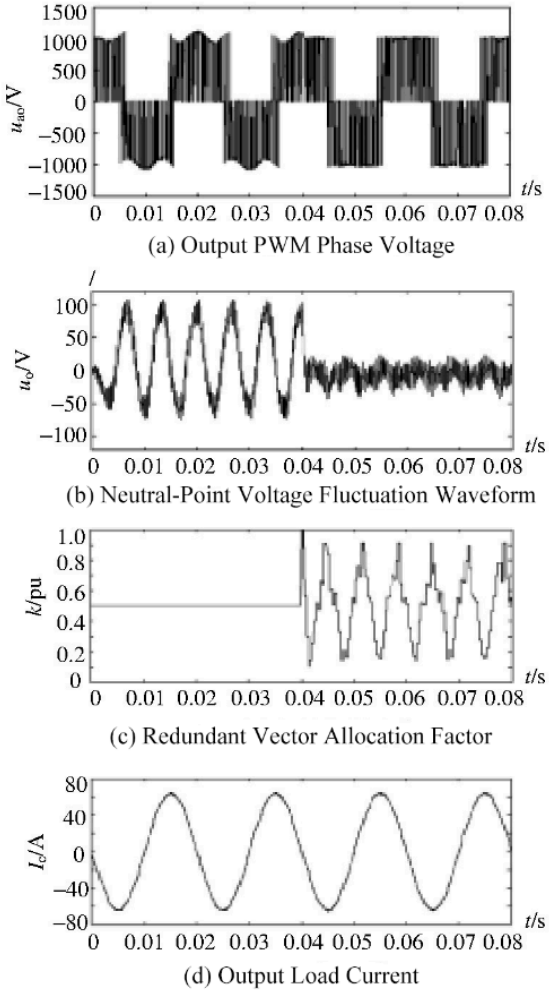

Figure 7. Simulation results for NP balancing control when M=0.8, f=50Hz [14]

2.2. Intermediate-stage DAB

For the intermediate-stage DAB converter, there are generally two control modes: DC voltage control and phase-shift control [15]. Phase-shift control includes Single Phase Shift (SPS), dual

DOI: 10.54254/2755-2721/2026.KA26760

phase-shift control, triple phase-shift control and extended phase-shift control.

The DC voltage control of DAB works as follows: DC is first converted into AC via full-bridge inversion, then passes through a high-frequency transformer, and is finally converted back to DC voltage via full-bridge rectification. Since the effective value of the AC output voltage of the full-bridge inverter can only be lower than the DC-side voltage, the voltage regulation range is greatly limited [16].

In phase-shift control, two full-bridge converters generate high-frequency square waves on the AC side. Ignoring excitation reactance, they can be equivalent to two current sources connected across an inductor. The magnitude and direction of power flow are adjusted by changing the phase shift [15]. This control method is widely used for its easy soft-switching implementation, small system inertia and fast dynamic response [17]. Common modulation methods for phase-shift control include single phase-shift, dual phase-shift, triple phase-shift and extended phase-shift.

The traditional Single Phase Shift (SPS) control features simple structure, but suffers from circulating power and is not applicable to DAB with mismatched input and output voltages [18, 19]. To solve this problem, scholars have carried out research from different perspectives. Reference [20] proposes a Dual Phase Shift (DPS) method for three-level converters, with phase shift realized on the primary side. Reference [21] puts forward a DPS control with phase shift only on one bridge arm side, which reduces return power, features smaller current stress and on-state loss at a given transmission efficiency, and improves transmission efficiency. Reference [22] presents a novel DPS control, which adds another degree of freedom to the system by adjusting the time sequence between gate signals of diagonal semiconductor switches. Compared with traditional phase-shift control, it delivers better dynamic and static performance, and can also limit the inrush current during startup. On this basis, Reference [23] establishes a mathematical model of current stress and conducts detailed quantitative analysis. Finally, experiments verify the correctness and superiority of the minimum current stress condition under all DPS modes, as well as the optimal current control principle and implementation scheme. Triple Phase Shift (TPS) control provides the maximum control freedom at a constant switching frequency by separately controlling the duty cycles of the two full bridges and the phase shift ratio between them. Thus, both SPS and DPS can be regarded as special cases of TPS. Reference [24] derives from the unified analysis of TPS control, takes all effective switching modes into account, and proposes a novel optimal modulation scheme based on TPS control to minimize current stress and achieve full soft-switching operation over the entire load range, formulating a unified implementation standard for DAB with TPS control.

3. Voltage and power balancing technologies for cascaded power electronic transformers

For PET with either MLCHB or MMC topology, the series multi-module structure may cause uneven voltage distribution at the input or output stage if any module has abnormally high or low voltage, resulting in local undervoltage or overvoltage, and even output distortion in severe cases. Meanwhile, both converters contain a large number of power devices, and inconsistent device parameters under synchronous control will also cause voltage drift. When different modules are controlled independently, accumulated errors from voltage sampling or control delay will also lead to voltage imbalance. The power imbalance of the intermediate-stage DAB is also one of the consequences of voltage imbalance [25]. Therefore, research on voltage and power balancing control strategies has always been a key and difficult point for the application of PET in various fields.

DOI: 10.54254/2755-2721/2026.KA26760

3.1. MMC

Since its proposal, MMC has been widely recognized for its modularity and scalability. In recent years, with the growing demand for long-distance power transmission, MMC has become the preferred topology in the HVDC field. However, MMC-HVDC faces the problem of DC-side short circuit. For small-capacity transmission, this can be solved by DC circuit breakers; but as capacity increases, the cost and manufacturing difficulty of DC circuit breakers rise sharply. Therefore, improved sub-modules (SM) are adopted in currently widely used MMC topologies to handle DC short circuits [26]. Based on this premise, this paper introduces the capacitor balancing control strategy of MMC.

Most literature adopts direct capacitor voltage balancing control: sort the capacitor voltages in the rectifier bridge arm, and switch the SM state to on at a specified time according to the sorting result and the direction of bridge arm current [27, 28]. Direct capacitor voltage balancing control has ideal dynamic performance, but it ignores the switching frequency requirement, leading to excessive switching frequency. Reference [29] optimizes the direct capacitor voltage balancing method. By comparing capacitor voltages, it identifies switch modules with higher capacitor voltages during the bridge arm current discharge period, and increases their probability of being switched on in the next switching cycle; correspondingly, the probability of other switch modules being switched off also increases. During the bridge arm current charging period, switch modules with lower capacitor voltages are set to be turned on in the next cycle, and SMs with capacitor voltages above the lower limit are more likely to be turned off. This method can quickly adjust capacitor voltages that exceed the limit, and maintain the switching state of modules within the safe range, thus reducing switching loss without significantly increasing capacitor voltage ripple amplitude. However, this method requires a large number of voltage sensors and sorting algorithms, and the huge data volume imposes pressure on the equipment. Reference [30] adopts the Nearest Level Control (NLC) method to simplify the method in Reference [29]. It sorts sub-modules according to the number of modules to be turned on, and generates gate pulses with the help of capacitor voltage switching states, thus saving 60% of the calculation amount [26]. The above are all active methods for capacitor voltage balancing, and there are also passive control methods. Reference [31] proposes to build an auxiliary circuit to realize voltage self-balancing. The auxiliary circuit consists of diodes and inductors, and the unbalanced energy of adjacent SM modules can be spontaneously transferred through the circuit. Meanwhile, the auxiliary circuit features low rated power, low loss and low cost. On this basis, Reference [26] proposes a novel sub-module with the function of outputting negative voltage levels, enabling MMC to handle DC short-circuit current. In summary, MMC voltage balancing strategies have been continuously optimized for simpler calculation and lower power consumption, and are dedicated to simultaneously solving difficulties in HVDC transmission according to application requirements.

3.2. MLCHB

The voltage and power balancing strategy for MLCHB-based PET can be directly realized via modulation technology. According to the spatial positions of triangular carriers, modulation technologies can be divided into Carrier Disposition (CD) and Carrier Phase Shift (CPS). Among these technologies, the PSC-PWM strategy features natural power balancing among cascaded H-bridge units [32], as well as low THD, high equivalent switching frequency, and uniform power and semiconductor stress distribution among SMs [33]. IPD-PWM is a variant of CPS-PWM. Under this modulation strategy, the output line voltage waveform has the minimum THD, but the different

DOI: 10.54254/2755-2721/2026.KA26760

switching time of each cascaded unit leads to different fundamental amplitude of output voltage and different output power of each cascaded H-bridge unit, resulting in uneven power distribution. Reference [34] proposes a hybrid multi-carrier PWM technology based on carrier reconstruction. It reconstructs the triangular carriers of the IPD-PWM strategy, increasing the switching function states from seven to eight (Figure 8). By utilizing redundant switching function states and adjusting the vertical arrangement of carriers, it changes the output voltage characteristics of H-bridge units while retaining the output level states, creating conditions for equal average output power of each cascaded unit. However, as the number of cascaded H-bridge units increases, the time required to achieve power balance becomes longer, and this strategy cannot improve DC-side voltage utilization.

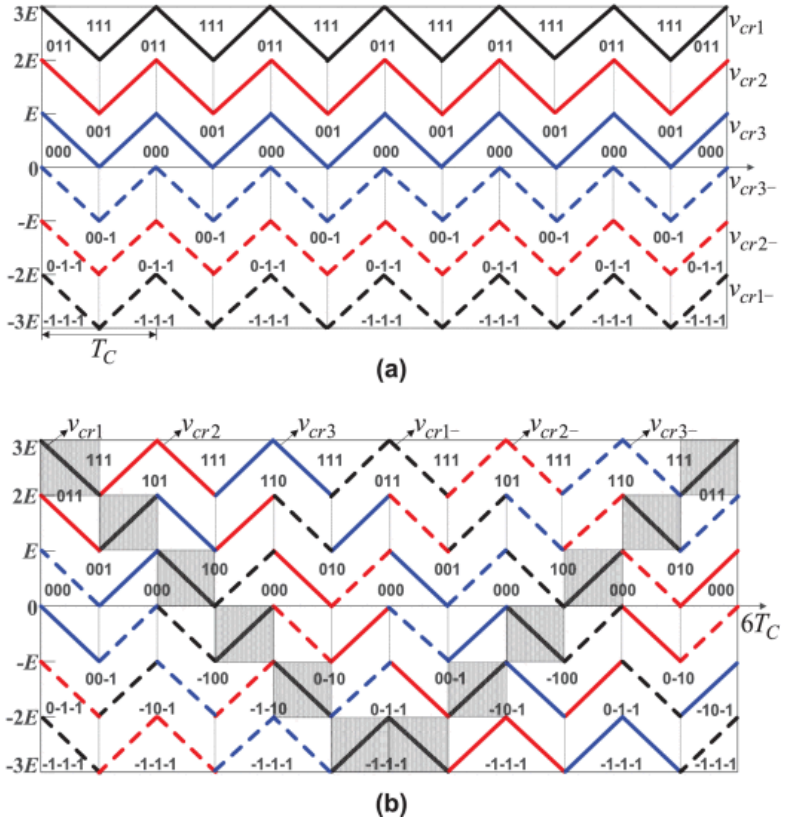

Figure 8. Carrier reconstruction diagram. (a) Before carrier reconstruction. (b) After carrier reconstruction [34]

Reference [35] proposes an IPD-TPWM strategy to address low DC-side voltage utilization and unbalanced output power among cascaded units. It replaces the sine wave in the traditional IPD-PWM strategy with a trapezoidal pulse width modulation signal. By verifying the relationship among DC voltage utilization, total harmonic distortion (THD) and triangulation rate δ, the optimal trapezoidal modulation wave is obtained. Meanwhile, the literature compares the output voltage waveform, phase voltage spectrum distribution and THD value of each unit under IPD-SPWM and IPD-TPWM strategies, verifying that this strategy increases DC voltage utilization by 19.1% and ensures power balance within the full modulation ratio range. The deficiency is that the literature does not compare the time required for the two strategies to achieve power balance.

DOI: 10.54254/2755-2721/2026.KA26760

4. Port control technologies for cascaded power electronic transformers

The output port of PET is usually directly connected to a load or a microgrid. For direct load connection scenarios such as locomotive traction systems and non-active distribution networks, providing voltage with stable frequency and amplitude is the main task of PET. Common port control strategies include V/F control, droop control, Virtual Synchronous Generator (VSG) control and variable frequency control. Droop control adjusts active and reactive power by imitating the parallel operation characteristics of synchronous generators. It was first proposed for Uninterruptible Power Supply (UPS) systems in Reference [36], and later became a general method for parallel inverters. Reference [37] introduces a control method for parallel inverter operation in islanded grids or infinite bus systems. It simulates a complex voltage source with finite output impedance by controlling the current flowing through the virtual impedance, which is caused by the voltage difference between the virtual AC source and the grid. This method is equivalent to droop control realized via modified active and reactive power. It can not only reduce voltage harmonics, but also control frequency and voltage more efficiently when line resistance cannot be ignored.

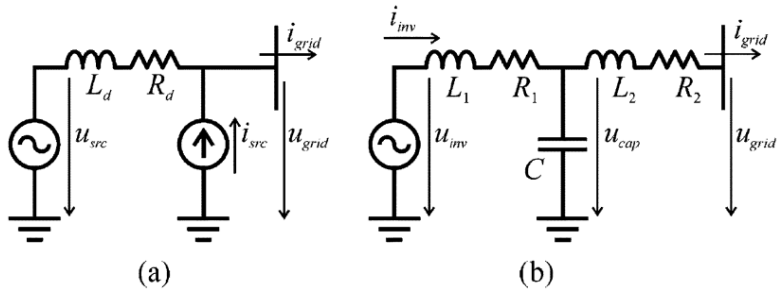

Figure 9. (a) virtual-system model; (b) real-system model [37]

In microgrid applications, droop control usually serves as the primary control in a hierarchical structure. The secondary control is used to keep frequency and voltage near nominal values, as well as to achieve accurate reactive power, harmonic and unbalanced power sharing [38].

However, since droop control cannot provide inertial support for the power system in distributed generation applications, the virtual synchronous generator method is proposed. In early VSG control technologies, VSG was mainly designed for energy storage devices rather than Distributed Generators (DG), with energy storage devices serving as dedicated frequency compensators [39, 40]. In recent years, VSG control methods for DG have also been gradually developed. Reference [41] improves traditional VSG control by removing slow components and main nonlinear components that affect synchronization speed and accuracy in the closed-loop system composed of synchronization unit, inverter controller and power system, and constructs a new controller. A common problem is that the above methods require a complete SG model in calculation, which makes the algorithm complex and usually occupies a large amount of processor capacity. Reference [42] extracts the basic elements of VSG and directly solves the rotor frequency through iteration of the swing equation, greatly reducing the calculation amount.

Reference [43] compares the dynamic characteristics of droop control and VSG control, and comprehensively analyzes the differences between the two control schemes caused by the swing equation.

DOI: 10.54254/2755-2721/2026.KA26760

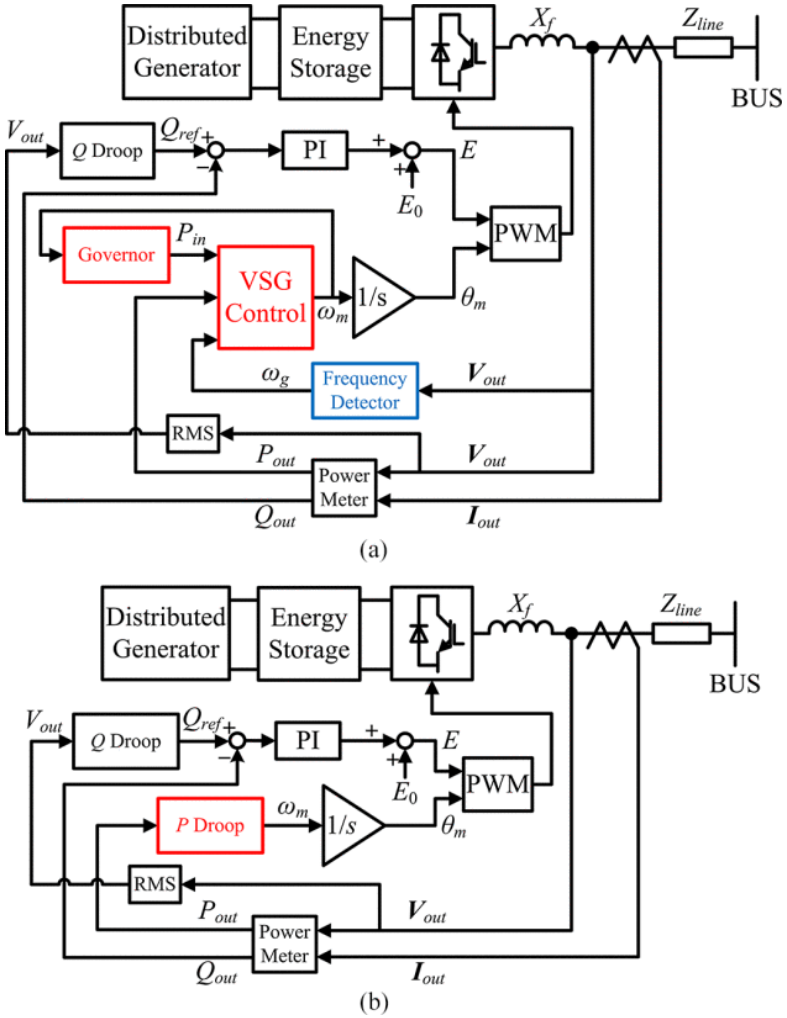

Figure 10. Basic control systems of (a) VSG and (b) droop control [43]

The literature establishes small-signal models of the two control modes in stand-alone operation mode and SG-connected mode, and calculates the step response of frequency change during load transition through the models.

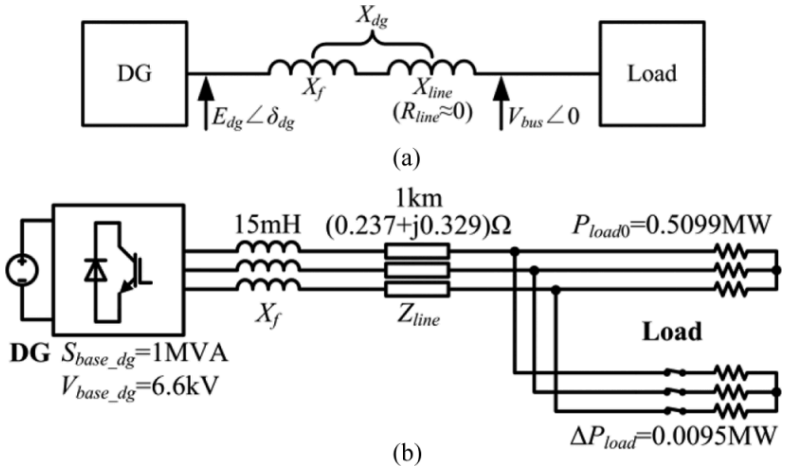

Figure 11. (a) Stand-alone mode model. (b) Simulation circuit of stand-alone mode [43]

DOI: 10.54254/2755-2721/2026.KA26760

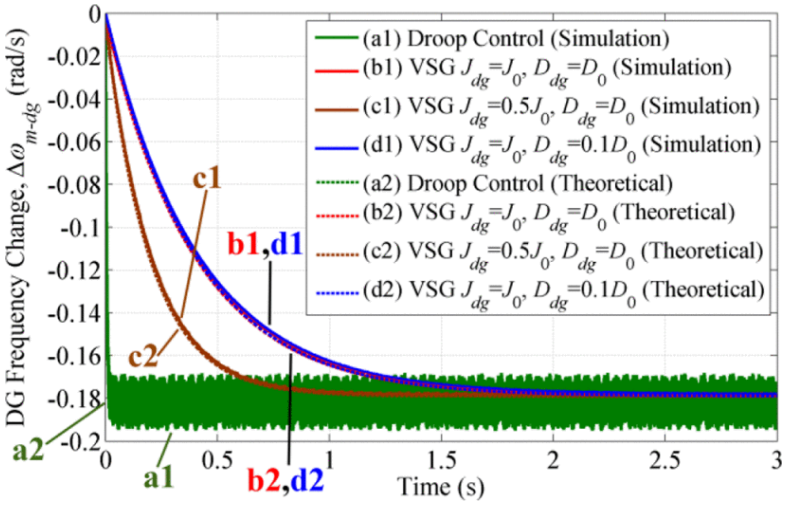

Figure 12. Step responses of DG frequency during a loading transition in standalone mode with various parameters [43]

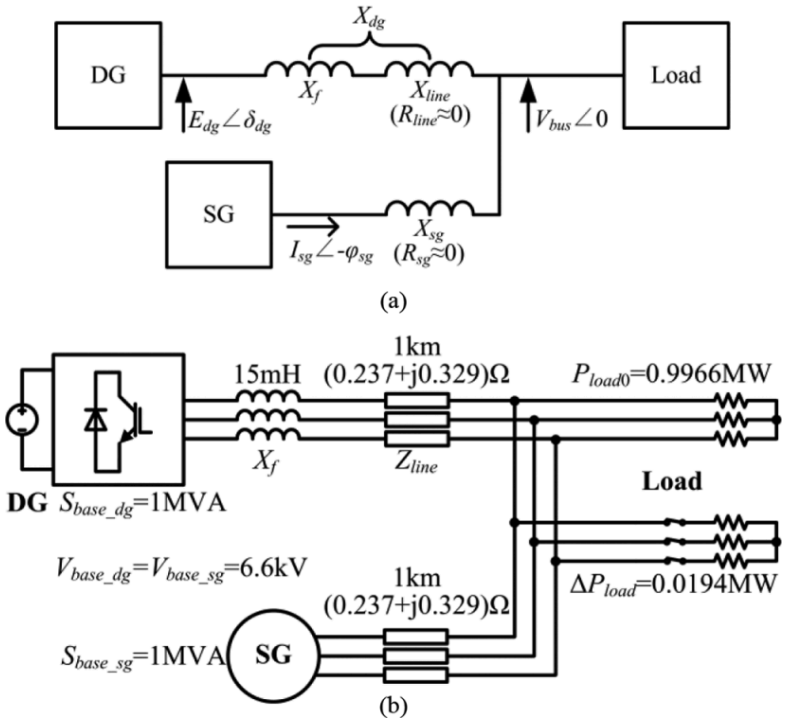

Figure 13. (a) SG-connected mode model. (b) Simulation circuit of SG-connected mode [43]

DOI: 10.54254/2755-2721/2026.KA26760

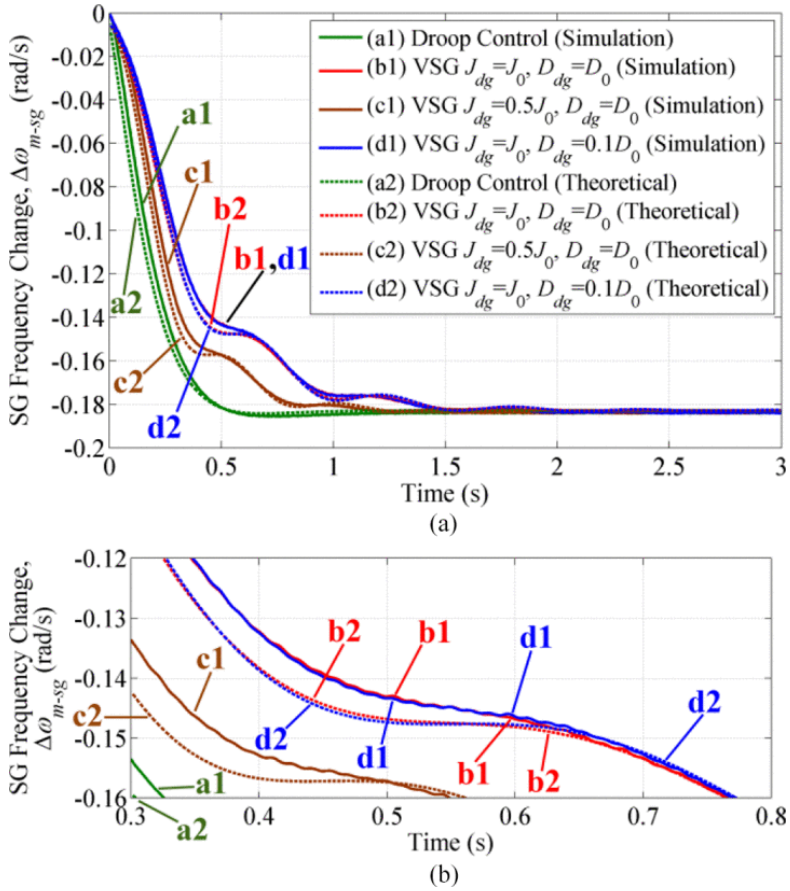

Figure 14. (a) Step responses of SG frequency during a loading transition in SG-connected mode with various parameters. (b) Zoom in of (a) [43]

Ripples can be observed in the droop control results during stand-alone mode simulation, and filters are required to eliminate ripples in practical applications. In terms of frequency change, DG with VSG control changes slowly, while DG with droop control has almost no inertia. The operation results in SG-connected mode are similar to those in stand-alone mode. The results show that distributed generators with droop control can contribute greater inertia to the system than those with VSG control, and the parameters of the swing equation have no impact on steady-state performance.

Next, the influence of delay effect from the governor and P droop controller on the two control methods is compared. When constructing the governor and P droop controller for the two methods, parameter replacement is required because the input and output are reversed in P-ω droop regulation. In VSG control, the output is active power and the input is frequency; in droop control, the input is active power and the output is frequency. According to the simulation results, delay makes the system frequency change faster under VSG control, while slower under droop control.

DOI: 10.54254/2755-2721/2026.KA26760

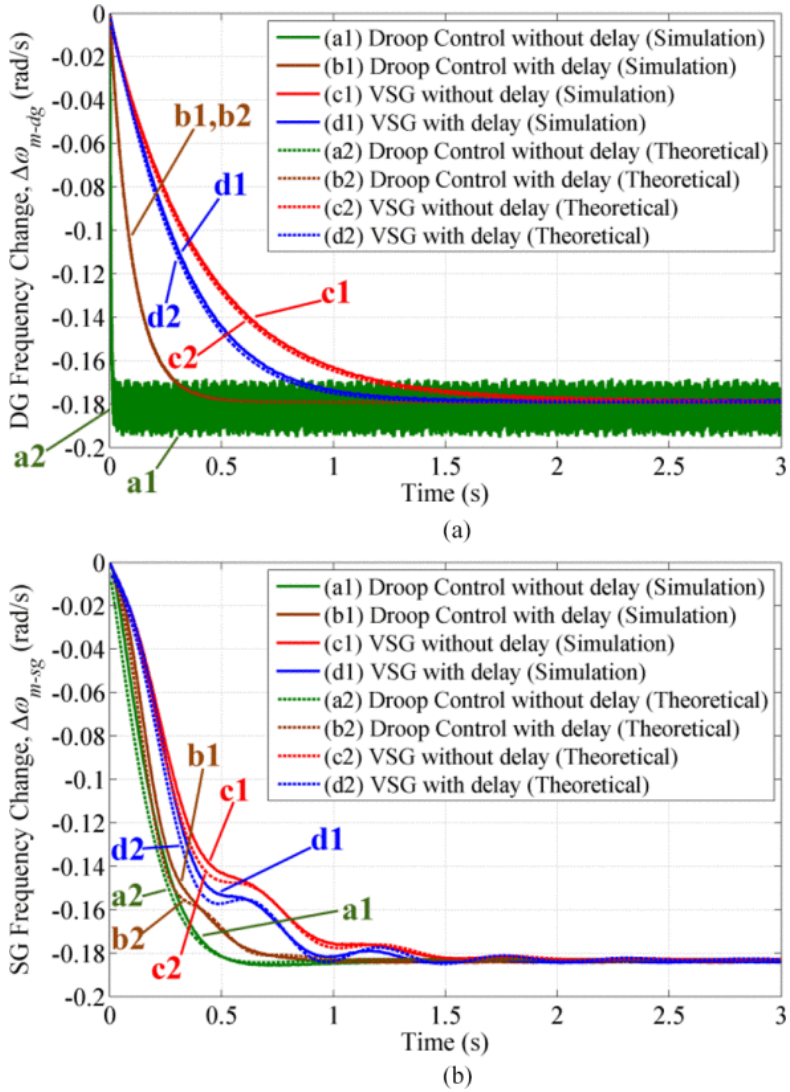

Figure 15. Effects of delays on step responses of (a) DG or (b) SG frequency during a loading transition in (a) stand-alone mode and (b) SG-connected mode [43]

5. Conclusion

This paper discusses the development status of cascaded PET from three aspects: modulation technology, voltage and power balancing strategies, and port control technologies. At present, cascaded PET shows broad application prospects in new energy grid integration, power transmission, rail transit and other fields for its modularity, high voltage adaptability and good scalability. Although current research has achieved many results, cascaded PET still faces many challenges in system stability, efficiency optimization and fault tolerance, such as inconsistent power module parameters, voltage imbalance and complex control systems. Based on a comprehensive analysis of the development process and existing technologies of cascaded PET, its future development directions are as follows:

(1) Topology optimization.

At present, MMC and MLCHB are the two most common topologies, but both have unsolved challenges. The modularity of MMC gives it irreplaceable advantages over other topologies in high-voltage adaptability, production, application, maintenance and expansion. However, a large number

DOI: 10.54254/2755-2721/2026.KA26760

of cascaded modules make the MMC-based cascaded PET system bulky and limited in practicability. While MLCHB improves fault tolerance and control flexibility by adding H-bridge structures, the system scale also expands rapidly, bringing great pressure to control coordination. Both topologies face the problem of complex and diverse control algorithms.

(2) Intelligent control for voltage and power balancing.

Most voltage and power balancing methods still rely on modulation technology to stabilize output voltage waveforms, or control the switching states of power devices. These control methods usually require huge calculation amount, and can only reduce losses by shutting down some or all modules when faults occur. Artificial intelligence algorithms have been fully developed in recent years. Technologies such as digital twin and reinforcement learning can be introduced to replace part of the calculation work of control strategy algorithms, reducing the computing pressure on controllers.

(3) Innovation of power device materials.

Cascaded PET contains a large number of power devices, and its control accuracy and output stability are highly dependent on these devices. Most PET damages are caused by overcurrent and overload of power devices. In the future development of PET, wide-bandgap devices made of semiconductor materials such as SiC and GaN can replace traditional IGBTs to improve the conversion efficiency and switching frequency of PET. Meanwhile, high-performance magnetic materials should be developed. At present, MnZn ferrite is the most common magnetic core material, with medium permeability, suitable for intermediate frequency conversion, low cost and mature technology. However, ferrite materials have low saturation magnetic flux density and large temperature drift, which greatly limit their application in high-frequency transformers. Nanocrystalline alloy is currently the most suitable material for high-frequency transformer magnetic cores. It has extremely low high-frequency loss, and can achieve the same induced voltage with a smaller volume, thus improving the power density of PET and reducing its overall size.

References

[1] Li, Z., Gao, F., Zhao, C., et al. (2018). A review of research on power electronic transformer technology. *Proceedings of the CSEE, 38*(5), 1274–1289. DOI:10.13334/j.0258-8013.pcsee.172575.

[2] Li, X., Hao, R., You, X., et al. (2017). A DC voltage balance control strategy for cascaded power electronic transformers. *Transactions of China Electrotechnical Society, 32*(2), 238–245. DOI:10.19595/j.cnki.1000-6753.tces.2017.02.027.

[3] Ronan, E. R., Sudhoff, S. D., Glover, S. F., & Galloway, D. L. (2000). Application of power electronics to the distribution transformer. *APEC 2000. Fifteenth Annual IEEE Applied Power Electronics Conference and Exposition (Cat. No.00CH37058)*, 861–867. DOI:10.1109/APEC.2000.822606.

[4] Xiao, F. (2018). *Research on optimal control and application of cascaded power electronic transformers*. Hunan University.

[5] Wang, S., Wang, Y., Lin, Y., et al. (2016). Voltage and power balancing control method for cascaded power electronic transformers. *Transactions of China Electrotechnical Society, 31*(22), 92–99. DOI:10.19595/j.cnki.1000-6753.tces.2016.22.012.

[6] Wang, S., Zhou, X., Tang, G., et al. (2011). Analysis of sub-module overcurrent under DC bipolar short circuit of modular multilevel converter HVDC. *Proceedings of the CSEE, 31*(1), 1–7. DOI:10.13334/j.0258-8013.pcsee.2011.01.001.

[7] Zhang, J. (2014). *Research on diode neutral-point clamped three-level inverter based on carrier modulation* [Doctoral dissertation, Huazhong University of Science and Technology].

[8] Li, Y., Gao, Y., & Hou, X. (2005). Current status and progress of PWM control technology for large-capacity multi-level converters. *Power Electronics*, (5), 5–9.

[9] Liu, Z., et al. (2022). Research on high frequency vibration reduction using carrier phase shifted PWM for 4-module 3-phase permanent magnet synchronous motor. *IEEE Transactions on Industry Applications, 58*(6), 7192–7200. https://doi.org/10.1109/TIA.2022.3198630

DOI: 10.54254/2755-2721/2026.KA26760

[10] Miyama, Y., et al. (2018). Vibration reduction by applying carrier phase-shift PWM on dual three-phase winding permanent magnet synchronous motor. *IEEE Transactions on Industry Applications, 54*, 5998–6004.
[11] Long, Q., Hu, L., Lu, B., et al. (2025). Analysis and suppression of abnormal increase of neutral line current in three-level H-bridge inverter considering high-frequency vibration suppression of multi-phase motors. *Proceedings of the CSEE*, 1–15. https://doi.org/10.13334/j.0258-8013.pcsee.242056
[12] Tu, Q., Xu, Z., & Xu, L. (2011). Reduced switching-frequency modulation and circulating current suppression for modular multilevel converters. *IEEE Transactions on Power Delivery, 26*(3), 2009–2017. https://doi.org/10.1109/TPWRD.2011.2115258
[13] Xiong, J., Kang, Y., Zhang, K., et al. (1999). Comparative study of voltage space vector modulation and conventional SPWM. *Power Electronics*, (1), 25–28.
[14] Song, W., Chen, G., Wu, H., et al. (2006). A three-level space vector modulation method with neutral-point potential balancing function and its implementation. *Proceedings of the CSEE*, (12), 95–100.
[15] Zhao, B., An, F., Song, Q., et al. (2021). Development and application of dual active bridge DC transformers. *Proceedings of the CSEE, 41*(1), 288–298+418. DOI:10.13334/j.0258-8013.pcsee.201635.
[16] Chung, I.-Y., et al. (2009). Integration of a bi-directional dc-dc converter model into a large-scale system simulation of a shipboard MVDC power system. In *2009 IEEE Electric Ship Technologies Symposium* (pp. 318–325). Baltimore, MD, USA. doi: 10.1109/ESTS.2009.4906531.
[17] Liu, D., & Li, H. (2006). A ZVS bi-directional DC–DC converter for multiple energy storage elements. *IEEE Transactions on Power Electronics, 21*(5), 1513–1517. doi: 10.1109/TPEL.2006.882450.
[18] De Doncker, R. W. A. A., Divan, D. M., & Kheraluwala, M. H. (1991). A three-phase soft-switched high-power-density DC/DC converter for high-power applications. *IEEE Transactions on Industry Applications, 27*(1), 63–73. doi: 10.1109/28.67533.
[19] Xie, Y., Sun, J., & Freudenberg, J. S. (2010). Power flow characterization of a bidirectional galvanically isolated high-power DC/DC converter over a wide operating range. *IEEE Transactions on Power Electronics, 25*(1), 54–66. https://doi.org/10.1109/TPEL.2009.2024151
[20] Zhang, Z., & Ruan, X. (2005). A novel double phase-shift control scheme for full-bridge three-level converter. *Twentieth Annual IEEE Applied Power Electronics Conference and Exposition, 2005. APEC 2005.* (pp. 1240–1245). https://doi.org/10.1109/APEC.2005.1453162
[21] Zhao, B., Yu, Q., & Sun, W. (2012). Analysis of power return characteristics of bidirectional full-bridge DC-DC converter with dual phase-shift control. *Proceedings of the CSEE, 32*(12), 43–50. https://doi.org/10.13334/j.0258-8013.pcsee.2012.12.008
[22] Bai, H., & Mi, C. (2008). Eliminate reactive power and increase system efficiency of isolated bidirectional dual-active-bridge DC–DC converters using novel dual-phase-shift control. *IEEE Transactions on Power Electronics, 23*(6), 2905–2914. https://doi.org/10.1109/TPEL.2008.2005103
[23] Wang, Y., Wang, S., Feng, B., et al. (2015). Optimal current control of dual active DC-DC converter based on dual phase-shift control. *Transactions of China Electrotechnical Society, 30*(14), 488–496. https://doi.org/10.19595/j.cnki.1000-6753.tces.2015.14.066
[24] Huang, J., Wang, Y., Li, Z., & Lei, W. (2016). Unified triple-phase-shift control to minimize current stress and achieve full soft-switching of isolated bidirectional DC–DC converter. *IEEE Transactions on Industrial Electronics, 63*, 4169–4179.
[25] Zheng, T., Wang, K., Zheng, Z., et al. (2022). A review of research on power electronic transformers based on MMC topology. *Proceedings of the CSEE, 42*(15), 5630–5649. DOI:10.13334/j.0258-8013.pcsee.220315.
[26] Huang, J., Li, K., Ye, Y., Wang, X., & Han, W. (2024). Novel hybrid modular multilevel converter with capacitor voltages self-balancing and DC-fault blocking abilities for MMC-HVDC. *IECON 2024 - 50th Annual Conference of the IEEE Industrial Electronics Society*, 1–6. https://doi.org/10.1109/IECON55916.2024.10905097
[27] Gemmell, B., Dorn, J., Retzmann, D., & Soerangr, D. (2008). Prospects of multilevel VSC technologies for power transmission. *2008 IEEE/PES Transmission and Distribution Conference and Exposition*, 1–16. https://doi.org/10.1109/TDC.2008.4517192
[28] Saeedifard, M., & Iravani, R. (2010). Dynamic performance of a modular multilevel back-to-back HVDC system. *IEEE Transactions on Power Delivery, 25*(4), 2903–2912. https://doi.org/10.1109/TPWRD.2010.2050787
[29] Guan, M., Xu, Z., & Chen, H. (2011). Control and modulation strategies for modular multilevel converter based HVDC system. *IECON 2011 - 37th Annual Conference of the IEEE Industrial Electronics Society*, 849–854. https://doi.org/10.1109/IECON.2011.6119421
[30] Meshram, P. M., & Borghate, V. B. (2015). A simplified nearest level control (NLC) voltage balancing method for modular multilevel converter (MMC). *IEEE Transactions on Power Electronics, 30*(1), 450–462. https://doi.org/10.1109/TPEL.2014.2317705

DOI: 10.54254/2755-2721/2026.KA26760

[31] Zheng, T., et al. (2021). A novel Z-type modular multilevel converter with capacitor voltage self-balancing for grid-tied applications. *IEEE Transactions on Power Electronics, 36*(2), 1399–1411. https://doi.org/10.1109/TPEL.2020.2997991

[32] Li, Y., Wang, Y., & Li, B. Q. (2016). Generalized theory of phase-shifted carrier PWM for cascaded H-bridge converters and modular multilevel converters. *IEEE Journal of Emerging and Selected Topics in Power Electronics, 4*(2), 589–605. https://doi.org/10.1109/JESTPE.2015.2476699

[33] Sekiguchi, K., Khamphakdi, P., Hagiwara, M., & Akagi, H. (2014). A grid-level high-power BTB (back-to-back) system using modular multilevel cascade converters without common DC-link capacitor. *IEEE Transactions on Industry Applications, 50*(4), 2648–2659. https://doi.org/10.1109/TIA.2013.2290867

[34] Ye, M., Chen, L., Kang, L., Li, S., Zhang, J., & Wu, H. (2019). Hybrid multi-carrier PWM technique based on carrier reconstruction for cascaded H-bridge inverter. *IEEE Access, 7*, 53152–53162. https://doi.org/10.1109/ACCESS.2019.2912216

[35] Ye, M., Ren, W., Chen, L., Wei, Q., Song, G., & Li, S. (2019). Research on power-balance control strategy of CHB multilevel inverter based on TPWM. *IEEE Access, 7*, 157226–157240. https://doi.org/10.1109/ACCESS.2019.2950064

[36] Chandorkar, M. C., Divan, D. M., & Adapa, R. (1993). Control of parallel connected inverters in standalone AC supply systems. *IEEE Transactions on Industry Applications, 29*(1), 136–143. https://doi.org/10.1109/28.195899

[37] De Brabandere, K., Bolsens, B., Van den Keybus, J., Woyte, A., Driesen, J., & Belmans, R. (2007). A voltage and frequency droop control method for parallel inverters. *IEEE Transactions on Power Electronics, 22*(4), 1107–1115. https://doi.org/10.1109/TPEL.2007.900456

[38] Micallef, A., Apap, M., Spiteri-Staines, C., Guerrero, J. M., & Vasquez, J. C. (2014). Reactive power sharing and voltage harmonic distortion compensation of droop controlled single phase islanded microgrids. *IEEE Transactions on Smart Grid, 5*(3), 1149–1158. https://doi.org/10.1109/TSG.2013.2291912

[39] Delille, G., Francois, B., & Malarange, G. (2012). Dynamic frequency control support by energy storage to reduce the impact of wind and solar generation on isolated power system's inertia. *IEEE Transactions on Sustainable Energy, 3*(4), 931–939. https://doi.org/10.1109/TSTE.2012.2205025

[40] Torres L., M. A., Lopes, L. A. C., Morán T., L. A., & Espinoza C., J. R. (2014). Self-tuning virtual synchronous machine: A control strategy for energy storage systems to support dynamic frequency control. *IEEE Transactions on Energy Conversion, 29*(4), 833–840. https://doi.org/10.1109/TEC.2014.2362577

[41] Zhong, Q.-C., Nguyen, P.-L., Ma, Z., & Sheng, W. (2014). Self-synchronized synchronverters: Inverters without a dedicated synchronization unit. *IEEE Transactions on Power Electronics, 29*(2), 617–630. https://doi.org/10.1109/TPEL.2013.2258684

[42] Alipoor, J., Miura, Y., & Ise, T. (2015). Power system stabilization using virtual synchronous generator with alternating moment of inertia. *IEEE Journal of Emerging and Selected Topics in Power Electronics, 3*(2), 451–458. https://doi.org/10.1109/JESTPE.2014.2362530

[43] Liu, J., Miura, Y., & Ise, T. (2016). Comparison of dynamic characteristics between virtual synchronous generator and droop control in inverter-based distributed generators. *IEEE Transactions on Power Electronics, 31*(5), 3600–3611. https://doi.org/10.1109/TPEL.2015.2465852